Supplement of Atmos. Chem. Phys., 26, 9471–9491, 2026
https://doi.org/10.5194/acp-26-9471-2026-supplement

Atmospheric Chemistry and Physics
Open Access
EGU

Supplement of

Intended and unintended consequences of atmospheric methane oxidation enhancement

Hannah M. Horowitz

Correspondence to: Hannah M. Horowitz (hmhorow@illinois.edu)

The Supplemental information contains the following: Figures S1-S6; Tables S1-S7; Section S1 (following Table S2)

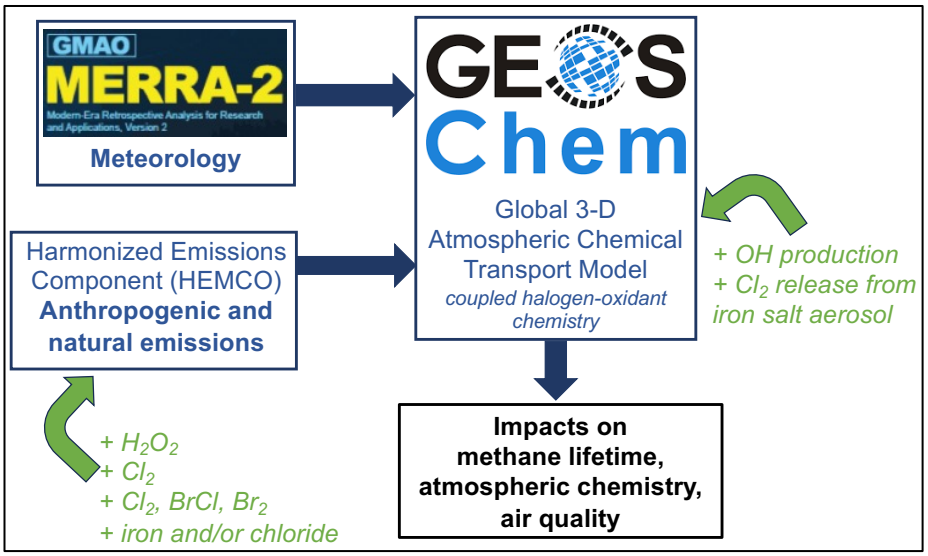

Figure S1. Methodology Schematic. The GEOS-Chem logo is provided for download at https://geoschem.github.io/logo.html (copyright © the International GEOS-Chem Community). The MERRA-2 logo was created by NASA's Global Modeling and Assimilation Office (GMAO) at NASA Goddard Space Flight Center (https://gmao.gsfc.nasa.gov/gmao-products/merra-2/).

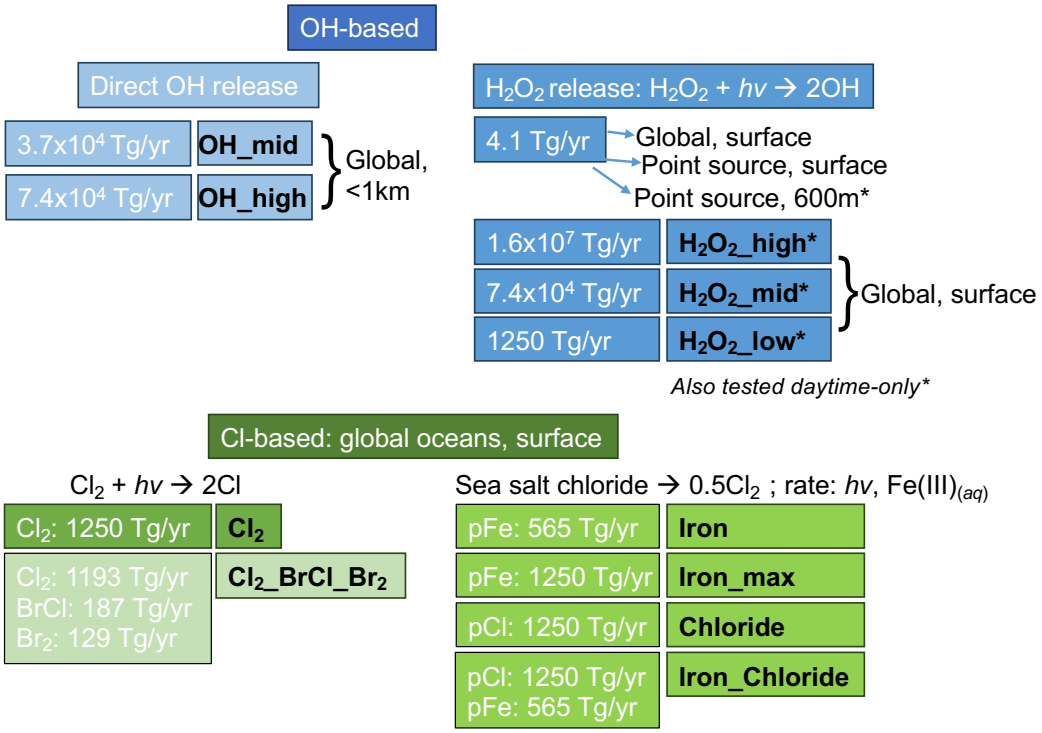

Figure S2. All model experiments conducted in the current study, grouped by methane oxidation mechanism and emitted species. pFe refers to particulate iron and pCl particulate accumulation-mode chloride.

S1. Additional details on calculations in the Chen et al. (2024) parameterization. Reaction rates given in the Wittmer et al. (2015b) Table 2 range from 6.6 – 8.7 × 10^{21} atoms $cm^{-2}hr^{-1}$ for artificial seawater and 8.7 – 13 × 10^{21} atoms cm^{-2} hr^{-1} for NaCl solution. Dividing by a factor of 3600 s/hr, the reaction rates are 1.8 – 2.4 × 10^{18} atoms $cm^{-2}s^{-1}$ for artificial seawater and 2.4 – 3.6 × 10^{18} atoms $cm^{-2}s^{-1}$ for NaCl solution. Wittmer et al. (2015b) summarized the rate as ~1.9 × 10^{18} atoms $cm^{-2}s^{-1}$ in the Abstract and Conclusions for a ratio of Cl^-/Fe^{3+} = 13. In Chen et al. (2024), from personal communication with Dr. Cornelius Zetzsch, this rate is incorrect as it was not adjusted for the volume of the chamber (requires dividing by the chamber size, 3.65 × 10^6). After the correction, the rate is reduced to 5.2 × 10^{11} atoms $cm^{-2}s^{-1}$ (as used in Chen et al., 2024).

The value of α (see Table 1 and Section 2.2.2.3) can be calculated from the reaction rates and aerosol surface areas provided in Wittmer et al. (2015b (See Table S3 below). Across this range of Cl^-/Fe^{3+} and aerosol surface areas, the values calculated for α are within 14%. Chen et al. (2024) uses the value of α calculated from the summary rate and Cl^-/Fe^{3+} ratio reported in the Abstract of Wittmer et al. (2015) rounded to two significant figures (α =1.4 × 10^5 μm^{-2} M^{-2}).

Table S1 Summary of Chen et al. (2024) parameter calculations from values in Wittmer et al. (2015b) and personal communication with Dr. Cornelius Zetzsch.

Cl^-/Fe^{3+}	**Reported rate (atoms $cm^{-2}s^{-1}$)**	**Corrected rate (atoms $cm^{-2}s^{-1}$)**	**Aerosol surface area concentration ($\mu m^2/cm^3$)**	**Calculated α (μm^{-2} M^{-2})**
13	1.9 × 10^{18}	5.2 × 10^{11}	30000	1.36 × 10^5
101	2.8 × 10^{17}	7.7 × 10^{10}	18000	1.55 × 10^5

Table S2 Comparison of Q. Li et al. (2023) and the Current Study Relevant to the Cl_2 and Cl_2_BrCl_Br_2 Scenarios

	Q. Li et al. (2023)	This Study
Model	CAM4-Chem-CESM-1.1	GEOS-Chem 13.2.1
Model run time	2020–2050	2019
Anthropogenic emissions	Representative concentration pathway 8.5 time-varying	CEDS CMIP6, year 2019
Halogen chemistry	Li et al. (2022); includes Saiz-Lopez et al. (2014) and Ordóñez et al. (2012) plus chlorine and bromine release from sea salt+N_2O_5 (also in GEOS-Chem), sea salt+HNO_3 (not in GEOS-Chem), and N_2O_5+HCl based on Hossaini et al. (2016)	Wang et al. (2021); includes Wang et al. (2019), Sherwen, Evans, et al. (2016), Sherwen, Schmidt, et al. (2016), and Zhu et al. (2019), plus sulfate formation from HOBr and HOCl, N_2O_5+Cl^- from Wang et al. (2020), improved reactive uptake coefficients on ice crystals for halogens
Model resolution	1.9° × 2.5° horizontal	4° × 5° horizontal
Model resolution	26 vertical levels up to 40 km	72 vertical layers up to 80 km; chemistry performed in first 59 layers up to 49.8 km

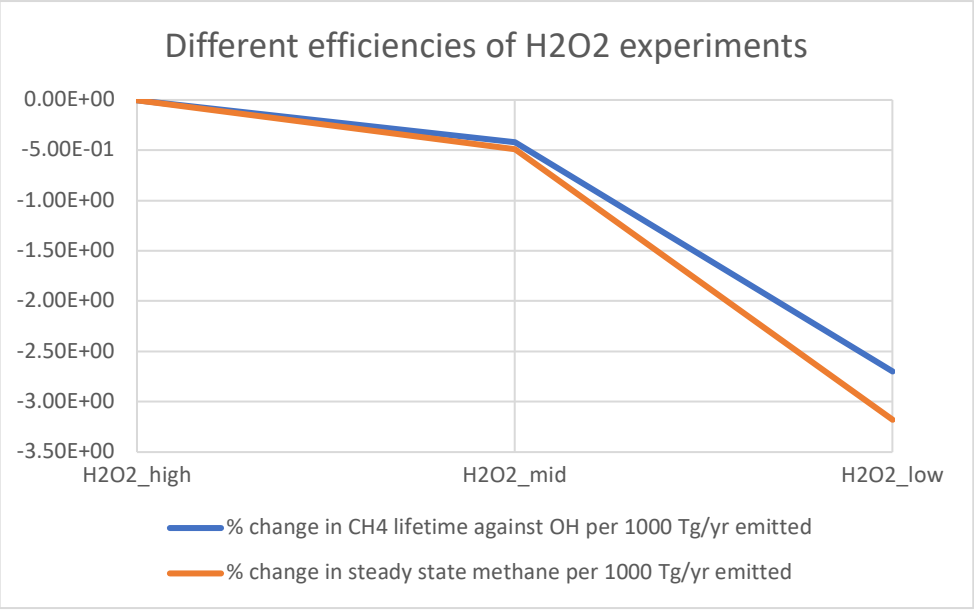

Figure S3 Normalized percent change in methane lifetime against oxidation by tropospheric OH (blue line) and change in steady-state methane concentration (orange line) per 1000 Tg/yr of H_2O_2 emissions across the three experiments detailed in Table 1.

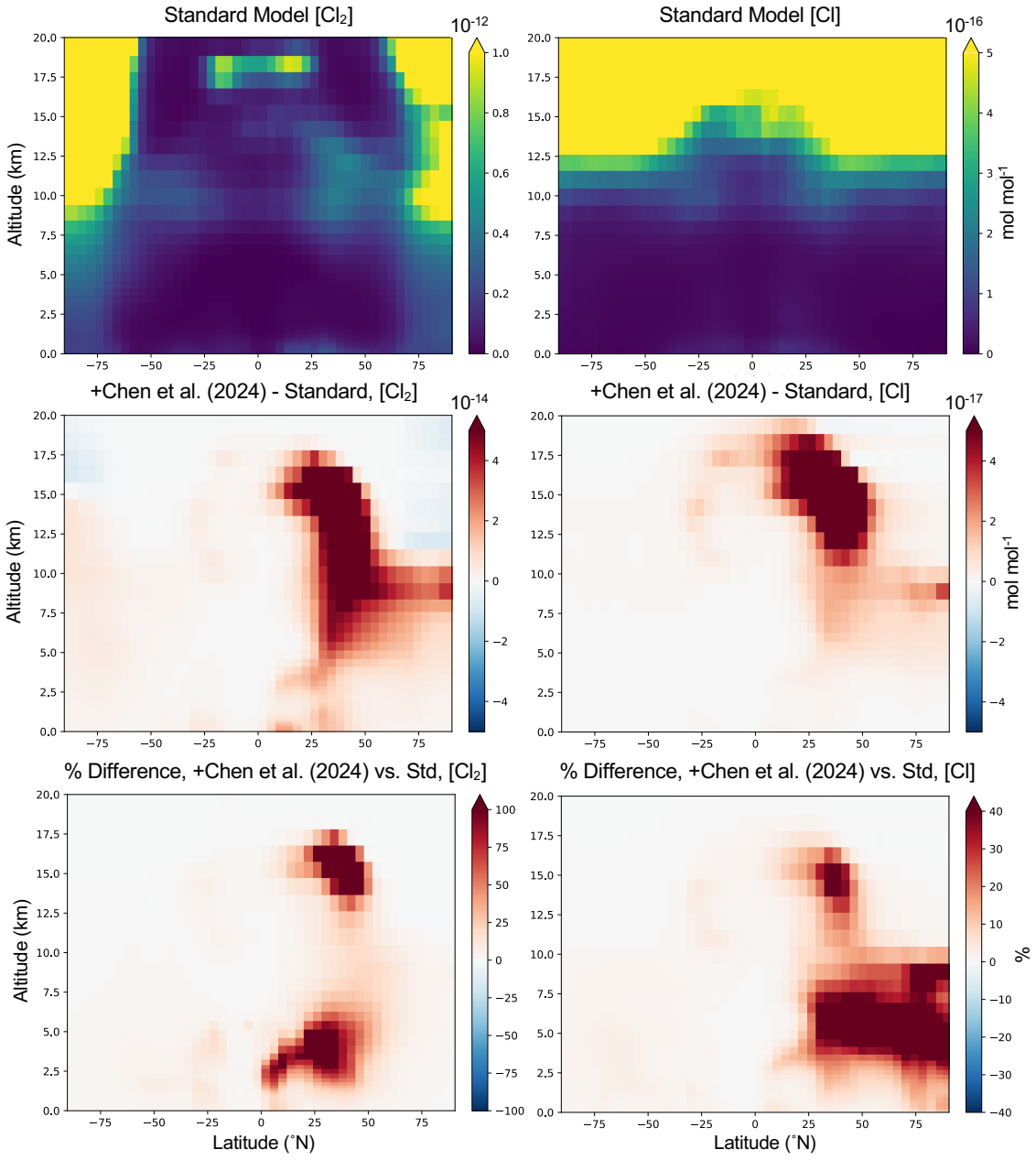

Figure S4: Impacts of adding natural Cl_2 emissions from the Chen et al. (2024) parameterization on simulated year 2019 zonal, annual mean concentrations of Cl_2 (left panels) and Cl (right panels) up to 20km altitude. The top row is the standard model concentrations (mol mol^{-1}), with the second and third rows containing the absolute difference in mol mol^{-1} and relative difference in percent, respectively, from adding the Chen et al. (2024) mechanism.

Table S3 Comparison of van Herpen et al. (2023) and Current Study for Iron and Chloride Scenarios

	van Herpen et al. (2023)	This Study
Model	CAM4-Chem	GEOS-Chem 13.2.1
Model run time	June 1996–1998	2019
Aerosols participating	Dust 1–2.5 μm	Dust 0.1–1 μm; Accumulation mode sea salt chloride (≤0.5 μm)
Dust iron content	3.5%	3.5%
Photoactive iron	Dust: 1.8%	Dust: 2.68% Anthropogenic*: 26.8%
Reaction rate for Cl_2 release	Fe(II)–Fe(III) cycling kinetics from Zhu et al. (1993) (calculations based on field samples)	Based on Wittmer, Bleicher, and Zetzsch (2015) chamber study (Chen et al., 2024)
Halogen chemistry	Wang et al. (2021)	Wang et al. (2021)
Horizontal model resolution	0.9° × 1.25°	4° × 5°
Vertical model resolution	56 vertical levels up to 40 km	72 vertical levels up to 80 km; chemistry performed in first 59 layers up to 49.8 km

**this includes pFe emitted in the Iron and Iron_Chloride AOE experiments*

Table S4 Selected reactions involving chlorine, bromine, and OH.

			Reaction rate (gas-phase) or reactive uptake coefficient γ (heterogeneous)	GEOS-Chem reference
OH reactions directly producing Cl and Cl_2				
†OH + Cl^-	→	0.5Cl_2 + OH^-	γ = 0.04[Cl^-]	Wang et al. (2019)
†OH + CH3Cl	→	Cl + HO2 + H2O	1.96E-12exp(-1200/T)	Eastham et al. (2014); updated to JPL 15-10
†OH + CH2Cl2	→	2Cl + HO2	2.61E-12exp(-944/T)	Sherwen et al. (2016)
†OH + CHCl3	→	3Cl + HO2	4.69E-12exp(-1134)	Sherwen et al. (2016)
†OH + CH3CCl3	→	3Cl + H2O	1.64E-12exp(-1520/T)	Eastham et al. (2014)
OH + HCFCs	→	*X*Cl + H2O*	Varies	Eastham et al. (2014); updated to JPL 15-10
Chlorine reactions producing CO				
CH2O + Cl	→	CO + HCl + HO2	8.1E-11exp(-30/T)	Sherwen et al. (2016)
CH3Cl + Cl	→	CO + 2HCl + HO2	2.17E-11exp(-1130/T)	Eastham et al. (2014); Sherwen et al. (2016)
CH2Cl2 + Cl	→	CO + HCl + 2Cl + HO2	1.24E-12exp(-1070/T)	Sherwen et al. (2016)
CHCl3 + Cl	→	CO + HCl + 3Cl + HO2	3.77E-12exp(-1011/T)	Sherwen et al. (2016)
Methane oxidation reactions				
CH4 + OH	→	CH3O2 + H2O	2.45E-12exp(-1775/T)	JPL 15-10
CH4 + Cl	→	CH3O2 + HCl	7.10E-12exp(-1270/T)	JPL 15-10

†*These reactions have an analogous equivalent involving bromine*

**X = 1 for HCFC22 and HCFC142b; X = 2 for HCFC141b and HCFC123.*

Table S5 Comparison of changes in tropospheric-wide Cl_2 and Cl burdens. Note: Percent change in annual mean tropospheric burdens for model experiments given in parentheses are relative to the standard version (* = relative to standard + Chen et al., 2024).

	Cl_2 (Gg)	ΔCl_2 (%)	Cl (kg)	ΔCl (%)	ΔCl_2/ΔCl ratio
Standard	1.06	--	313	--	--
Cl2	926.7	87369.7%	7250	2213.6%	39.5
Cl2_BrCl_Br2	829.7	78216.5%	6171	1869.5%	41.8
Standard+Chen	1.16	9.8%	343	9.4%	1.0
Iron*	14.04	1107.6%	924	169.4%	6.5
Chloride*	3.99	243.2%	955	178.6%	1.4
Iron_Chloride*	34.30	2849.4%	2599	658.0%	4.3

Table S6 Percent Changes in Tropospheric Burdens for the OH Experiments

	Br_y	Cl_y	I_y	O_3	OH	Cl	NO_x	CO
Standard	20 Gg	241 Gg	12 Gg	338 Tg	215 Mg	318 kg	359 Gg	349 Tg
OH_mid	41.2%	11.6%	-17.8%	-10.4%	50.8%	45.2%	-21.1%	-26.4%
OH_high	54.6%	19.5%	-28.3%	-14.3%	94%	72.3%	-24.7%	-31.1%

TABLE S7 Percent Change in Tropospheric Burdens of Other Climate Forcers and Ozone-Depleting Substances, with Cl Atom Included for Reference, for Experiments Described in Table 1

	HCFC-123 (%)	Total inorganic aerosol (%)	Dibromo-methane (CH_2Br_2) (%)	Bromoform ($CHBr_3$) (%)	Methyl ioidide (CH_3I) (%)	Cl (%)	Ozone (%)
H2O2_high	-74.2	10.1	-59.5	-39.4	-6.6	401.7	-38.5
H2O2_mid	-34.8	12.6	-30.9	-20.9	-3.0	73.8	-6.0
H2O2_low	-3.9	6.4	-3.9	-2.6	-0.4	6.3	-0.7
Cl2	30.7	6.7	35.5	10.8	-1.1	2213.6	-24.4
Cl2_BrCl_Br2	62.6	20.2	80.5	11.9	-7.8	1869.5	-67.1
Iron	2.6	9.1	2.7	1.0	-0.2	169.4	-3.4
Chloride	5.4	-0.6	5.6	2.3	-0.2	178.6	-5.6
Iron_Chloride	10.9	10.1	11.7	4.4	-0.5	658.0	-10.6

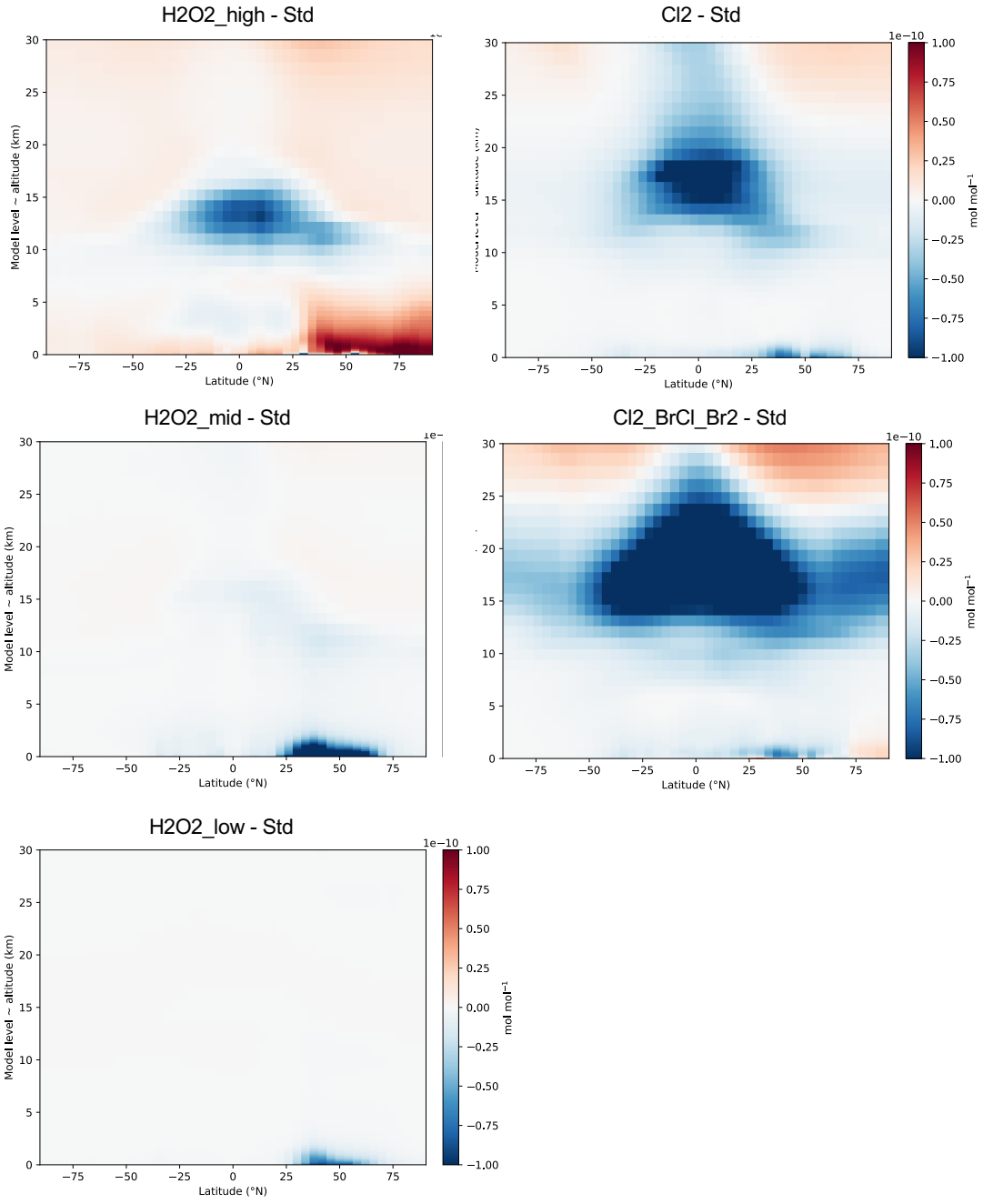

Figure S5 Zonal mean absolute changes in NO_x across the scenarios in mol/mol.

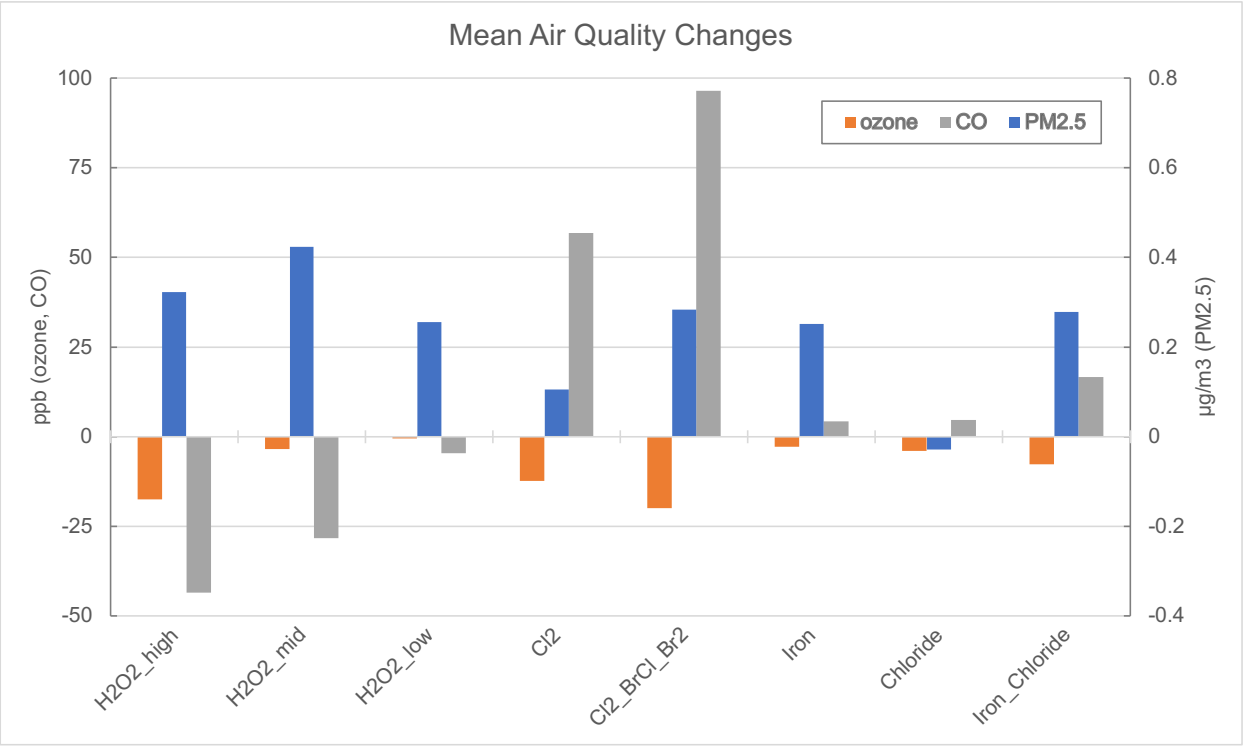

Figure S6 Changes in global annual mean ozone (orange), CO (gray) (left axis), and $PM_{2.5}$ (blue, right axis) concentrations across the experiments.

80

Additional References

Li, Q., Fernandez, R. P., Hossaini, R., Iglesias-Suarez, F., Cuevas, C. A., Apel, E. C., Kinnison, D. E., Lamarque, J.-F., and Saiz- Lopez, A.: Reactive halogens increase the global methane lifetime and radiative forcing in the 21st century, Nat. Commun., 13, 2768, https://doi.org/10.1038/s41467-022-30456-8, 2022.

Ordóñez, C., Lamarque, J.-F., Tilmes, S., Kinnison, D. E., Atlas, E. L., Blake, D. R., Sousa Santos, G., Brasseur, G., and Saiz-Lopez, A.: Bromine and iodine chemistry in a global chemistry-climate model: description and evaluation of very short-lived oceanic sources, Atmos. Chem. Phys., 12, 1423– 105 1447, https://doi.org/10.5194/acp-12-1423-2012, 2012.

Saiz-Lopez, A., Fernandez, R. P., Ordóñez, C., Kinnison, D. E., Gómez Martín, J. C., Lamarque, J.-F., and Tilmes, S.: Iodine chemistry in the troposphere and its effect on ozone, Atmos. Chem. Phys., 14, 13119–13143, https://doi.org/10.5194/acp-14- 13119-2014, 2014.

Sherwen, T., Evans, M. J., Carpenter, L. J., Andrews, S. J., Lidster, R. T., Dix, B., Koenig, T. K., Sinreich, R., Ortega, I., Volkamer, R., Saiz-Lopez, A., Prados-Roman, C., Mahajan, A. S., and Ordóñez, C.: Iodine's impact on tropospheric oxidants: a global model study in GEOS-Chem, Atmos. Chem. Phys., 16, 1161–1186, https://doi.org/10.5194/acp-16-1161-2016, 2016a.

Wang, X., Jacob, D. J., Fu, X., Wang, T., Breton, M. L., Hallquist, M., Liu, Z., McDuffie, E. E., and Liao, H.: Effects of anthropogenic chlorine on PM2.5 and ozone air quality in China, Environ. Sci. Technol., 54, 9908–9916, https://doi.org/10.1021/acs.est.0c02296, 2020.

Zhu, L., Jacob, D. J., Eastham, S. D., Sulprizio, M. P., Wang, X., Sherwen, T., Evans, M. J., Chen, Q., Alexander, B., Koenig, T. K., Volkamer, R., Huey, L. G., Le Breton, M., Bannan, T. J., and Percival, C. J.: Effect of sea salt aerosol on tropospheric bromine chemistry, Atmos. Chem. Phys., 19, 6497–6507, https://doi.org/10.5194/acp-19-6497-2019, 2019.